Theoretical Study of the $HS(v', j' = 1) + O_2(v'' = 0, j'' = 1)$ Reaction

M. Y. BALLESTER,[1] Y. O. GUERRERO,[2] J. D. GARRIDO[2]

[1]*Departamento de Química, Universidade de Coimbra, Portugal*

[2]*Departamento de Física General y Matemáticas, Instituto Superior de Tecnología y Ciencias Aplicadas Habana, Cuba*

Received 10 October 2007; accepted 28 November 2007
Published online 22 January 2008 in Wiley InterScience (www.interscience.wiley.com).
DOI 10.1002/qua.21591

ABSTRACT: We report a theoretical study of the title four-atom reaction for a wide range of translational energies, considering the reactants in the ground vibrational state and also in some vibrationally excited levels of the HS radical. All calculations have employed the quasi-classical trajectory (QCT) method and a reported double many-body expansion potential energy surface for ground electronic state of HSO_2. Cross sections as well as specific rate constants for HS elimination are reported and compared with literature data for such processes. To account the zero-point energy problem in QCT calculations, an internal energy quantum mechanics threshold (IEQMT) criteria is used.

Key words: reaction dynamics; sulfur; atmospheric reactions

1. Introduction

The importance of sulfur as a major contaminant in different environmental issues such as acid rain, air pollution, and global climate changes has been well established. It comes both from natural and anthropogenic sources [1]. Its influence is not limited to the troposphere because some compounds, as COS, may reach the stratosphere and there can enter into different chemical cycles [1]. The production of HS radical from photolysis [2–8]

$$H_2S + h\nu \rightarrow HS(X\,^2\Pi, v) + H \qquad (1)$$

and reaction

$$H_2S + OH \rightarrow HS + H_2O \qquad (2)$$

Correspondence to: J. D. Garrido; e-mail: garrido.jd@gmail.com
This work was presented at the XXXIII QUITEL conference held in September 2007 in Havana, Cuba.
Contract grant sponsor: Fundação para a Ciência e a Tecnologia (FCT) de Portugal.
Contract grant number: SFRH/BD/4777.
Contract grant sponsor: Third World Academy of Science (TWAS).
Contract grant number: 97-144, RG/CHE/LA.
Contract grant sponsor: German Academic Exchange Service (DAAD).

are well-established processes [1, 9], but the fate of the produced HS radical is less clear, and therefore appears the necessity to understand the subsequent oxidation steps to elucidate the route leading to different contaminant environmental events. Between the possible channels leading to the loss of HS radical, one of the main issues is the reaction

$$HS + O_2 \rightarrow \text{products}. \quad (3)$$

Experimentally, reaction (3) has been studied in several works [10–16], but measurements have yielded only upper limits that fall in the range of 4×10^{-19} to 1×10^{-14} $cm^3\,s^{-1}$ at 298 K (the preferred value by IUPAC Subcommittee on Gas Kinetic Data Evaluation [15] is 4×10^{-19} $cm^3\,s^{-1}$). For high translational temperature ($1{,}400 \leq T\ (K) \leq 1{,}850$) a dependence with temperature for rate constant of reaction (3), $k(T) = 3.1 \times 10^{-11} \exp(-75\ kJ\,mol^{-1}/RT)$ $cm^3\,s^{-1}$, has been proposed in Ref. 17. A further analysis about these experimental results will be done later.

From the theoretical side, there are some studies of the HSO_2 isomers using ab initio calculations at different levels of theory [18–27] and also by means of DFT [28]. Recently the first global potential energy surface (PES) for the mentioned system was reported [29]. Even when theoretical works [18, 27, 30] have reported rate constants for reaction (3), none of them have used a global PES and showed significant differences in their calculated values. Thus, it is very interesting to carry out calculations to determinate the rate constants of the title reaction using such a PES [29]. Moreover, the global PES allows to carry out calculations for vibrationally excited states of the electronic ground state of reactants, probably a relevant fact for comparison with experiments and for atmospheric chemistry.

Despite vibrationally excited molecules could have an important role in the interpretation of experimental results and in the atmospheric physicochemical modeling, it is not common to find in the literature theoretical studies devoted to the analysis of the effect of internal energy of reactants on chemical reactions. In particular, to our knowledge, no single study of reaction (3) considering vibrationally excited reactants has been reported. A major goal of the present work is therefore to report a quasiclassical trajectory (QCT) study of the reactions:

$$HS(v', j = 1) + O_2(v'' = 0, j'' = 1) \rightarrow \text{products} \quad (4)$$

with different vibrational states (v' for HS radical). For this purpose, we employ a realistic single-valued double many-body-expansion (DMBE) PES [29] for the electronic ground state of HSO_2. Such a methodology should be reliable since the QCT approach treats the problem in its full dimensionality and most of the involved nuclei are heavy. Furthermore, one is interested to carry out calculations for several vibrational levels combinations and the treatment of such a problem with quantum reaction dynamic calculations is virtually prohibitive. The paper is organized as follows. Section 2 provides a brief survey of the HSO_2 potential energy surface, whereas the computational method is described in Section 3. The results are presented and discussed in Section 4, whereas the major conclusions are gathered in Section 5.

2. Potential Energy Surface

All calculations in this work have employed a six-dimensional (6D) DMBE [31] PES for the electronic ground state of HSO_2. It employs DMBE functions previously reported for the diatomic and triatomic fragments (see Ref. 29 and references therein) and four-body energy terms to mimic ab initio CASPT2/FVCAS/AVXZ ($X = 2, 3$) calculations for the tetratomic system. Since it has already been described in detail elsewhere [29], we focus here on its main topographical features which are of interest for the title reaction.

Minimum energy path for formation of HSO is presented in Figure 1. For simplicity, the same

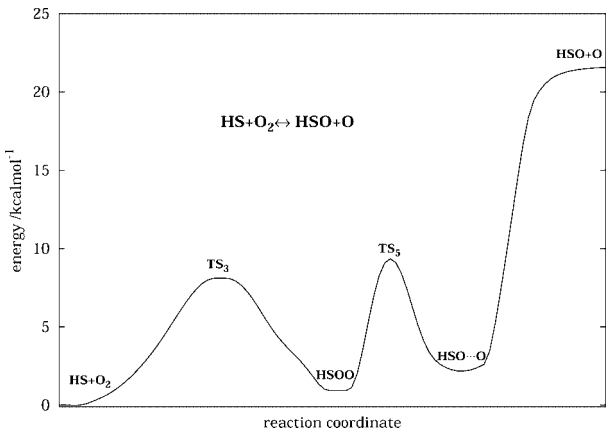

FIGURE 1. Minimum energy path for the reaction $HS + O_2 \rightarrow HSO + O$, according to the global PES of HSO_2 used in this work.

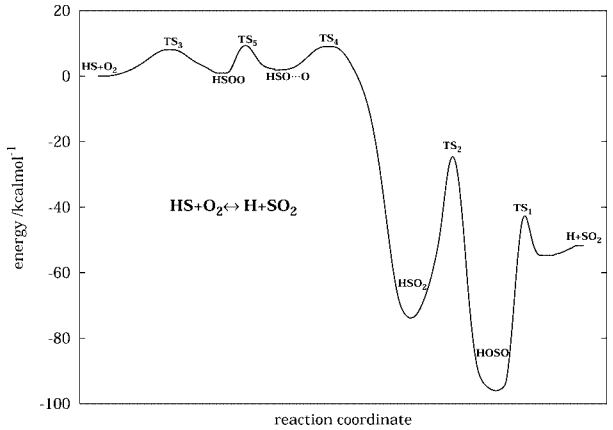

FIGURE 2. Minimum energy path for the reaction $HS + O_2 \rightarrow H + SO_2$, according to the global PES of HSO_2 used in this work.

nomenclature given in a previous paper [29] is used. Thus, TS_3 labels the transition state for the formation of HSOO from $HS + O_2$, TS_5 defines the barrier for isomerization $HSOO \rightarrow HSO \cdots O$. Figure 2 displays the minimum energy path for the reaction $HS + O_2 \rightarrow H + SO_2$. TS_4 is the intermediate state between $HSO \cdots O$ and HSO_2, whereas TS_2 is for isomerization $HSO_2 \rightarrow HOSO$ (the possible way $HSO_2 \rightarrow H + SO_2$ has not been shown in the figure). Although other species may be obtained as products, the above mentioned ones are the more likely to occur under the selected conditions of the present work (see later).

3. Computational Procedures

QCT method [32] has been used to study the title reaction. To run the classical trajectories we have utilized an adapted version of the VENUS96 [33] code which accommodates the HSO_2 DMBE potential energy surface, described in the previous section. Calculations have been carried for diatom–diatom translational energies in the range $10 \leq E_{tr}$ (kcal mol^{-1}) ≤ 40, as specified in Table I. In all cases, the initial rotational quantum number of the colliding HS and O_2 molecules have been fixed at their ground level ($j'_{HS} = j''_{O_2} = 1$) and the O_2 molecule kept in its ground vibrational state. The step size of the numerical integrations was 2.5×10^{-16} s, warranting conservation of the energy better than two parts into 10^5. In turn, diatomic–diatomic initial separation have been fixed at 9 Å, a value sufficiently large to make the interaction negligible. To select the maximum value of the impact parameter (b_{max}) which leads to reaction, we have followed the usual procedure by computing batches of 300 trajectories for fixed values of b. This procedure should allow an accuracy in b_{max} of about ±0.1 Å; the calculated values are reported in the third column of Table I. Considering the energetic barriers of the PES for title reaction, batches of 5,000 trajectories have been then run for each translational energy and vibrational combination making a total of about 1.75×10^5 trajectories. Such a number of trajectories has been found enough to yield reactive cross sections with an error of typically a few percent. The procedure employed to assign reactive channels is identical to that reported in previous works [34, 35] for other reactive system: when a trajectory reach a configuration corresponding to an specific channel, a product is considered to be formed, and the trajectory is therefore ended. Diatom–diatom collisions may lead to 14 possible channels. As before [36], we do not consider as distinct channels the various isomers of a given species.

For a given value of the translational energy, the specific reactive cross section for HS lost (or specific total reactive cross section) assumes the form [37]

$$\sigma^r_{v',0} = \pi b^2_{max} P^r_{v',0} \tag{5}$$

with the associated uncertainties being given by [37]

$$\Delta\sigma^r_{v',0} = \left(\frac{N_{v',0} - N^r_{v',0}}{N_{v',0} N^r_{v',0}} \right)^{1/2} \sigma^r_{v',0} \tag{6}$$

where $N^r_{v',0}$ denotes the number of reactive trajectories in a total of $N_{v',0}$ for the combination $(v', 0)$ of the vibrational quantum numbers of the colliding molecules, and $P^r_{v',0} = N^r_{v',0}/N_{v',0}$ is the corresponding reactive probability. From the specific total reactive cross section and assuming a Maxwell–Boltzmann distribution over the translational energy (E_{tr}), the specific thermal total reactive rate coefficient is obtained as

$$k^r_{v',0}(T) = g_e(T) \left(\frac{2}{k_B T} \right)^{3/2} \left(\frac{1}{\pi \mu} \right)^{1/2} \times \int E_{tr} \sigma^r_{v',0} \exp\left(-\frac{E_{tr}}{k_B T} \right) dE_{tr}, \tag{7}$$

where $g_e(T) = \frac{1}{3}[1 + \exp(-544.7/T)]^{-1}$ is the appropriate electronic degeneracy factor [38, 39]. Notice

TABLE I

Trajectories calculation results for the reaction $HS(v', 1) + O_2(0, 1)$.

v'	E_{tr}[a]	b_{max}	N_T^{IEQMT}	N_r^{IEQMT}	N_r^{QCT}	σ_{IEQMT}^r	$\Delta\sigma_{IEQMT}^r$	σ_{QCT}^r	$\Delta\sigma_{QCT}^r$
0	20.0	0.6	3,774	54	54	0.016	0.002	0.012	0.002
	22.5	1.3	4,075	23	25	0.030	0.006	0.027	0.005
	24.0	1.3	3,980	38	46	0.051	0.008	0.049	0.007
	28.0	1.5	4,013	73	78	0.129	0.015	0.110	0.012
	32.0	1.6	4,168	109	111	0.210	0.020	0.179	0.017
	36.0	1.7	4,061	201	204	0.450	0.030	0.370	0.025
	40.0	1.8	4,165	310	310	0.758	0.041	0.631	0.035
	45.0	1.8	4,221	547	547	1.319	0.053	1.114	0.044
1	17.5	0.8	4,137	9	9	0.004	0.001	0.004	0.001
	20.0	1.2	4,297	25	25	0.026	0.005	0.226	0.005
	25.0	1.6	4,425	44	44	0.080	0.012	0.071	0.011
	30.0	1.8	4,508	96	96	0.217	0.022	0.195	0.020
	40.0	2.0	4,619	264	264	0.718	0.043	0.664	0.040
	45.0	2.0	4,621	390	390	1.061	0.051	0.982	0.048
3	12.5	0.3	4,384	17	17	0.0011	0.0003	0.0096	0.0002
	15.0	1.4	4,507	7	7	0.0096	0.0004	0.009	0.003
	17.5	1.4	4,327	24	24	0.034	0.007	0.030	0.006
	20.0	1.6	4,410	29	29	0.053	0.010	0.047	0.009
	25.0	1.9	4,488	64	64	0.162	0.020	0.145	0.018
	30.0	1.8	4,525	119	121	0.268	0.024	0.246	0.022
	40.0	1.9	4,569	303	303	0.752	0.042	0.687	0.038
	40.0	1.9	4,569	303	303	0.752	0.042	0.687	0.038
	45.0	2.1	4,625	353	353	1.057	0.054	0.978	0.050
5	12.5	1.3	4,219	29	32	0.036	0.007	0.034	0.006
	15.0	1.4	4,332	49	49	0.070	0.010	0.060	0.009
	17.5	1.6	4,352	49	49	0.091	0.013	0.079	0.011
	20.0	1.7	4,328	64	64	0.134	0.017	0.116	0.014
	22.5	1.7	4,450	100	100	0.204	0.020	0.182	0.018
	25.0	2.0	4,450	84	84	0.237	0.026	0.211	0.023
	30.0	2.2	4,519	122	122	0.411	0.037	0.371	0.033
	40.0	2.0	4,623	386	388	1.049	0.051	0.975	0.048
	45.0	2.1	4,687	509	509	1.505	0.063	1.410	0.059
7	10.0	1.5	3,870	18	18	0.033	0.008	0.025	0.006
	15.0	1.8	4,002	38	38	0.097	0.016	0.077	0.013
	20.0	2.0	4,307	103	105	0.301	0.029	0.264	0.025
	25.0	2.2	4,434	271	271	0.929	0.051	0.814	0.049
	30.0	2.0	4,592	630	630	1.724	0.064	1.583	0.059
	35.0	2.1	4,663	762	765	2.264	0.075	2.119	0.070
	40.0	2.2	4,730	852	859	2.739	0.085	2.612	0.080

[a] In kcal mol^{-1}.

that $HS(^2\Pi)$ split into two double-fold degenerate states [$HS(^2\Pi_{1/2})$ and $HS(^2\Pi_{3/2})$] when first-order spin-orbit interaction is considered, with 544.7 K of energy difference between them [40]. $O_2(^3\Sigma)$ is a triplet whereas the complex is a doublet, k_B is the Boltzmann constant, μ is the reduced mass of the colliding diatomic particles, and T is the temperature.

4. Results and Discussion

4.1. REACTIVE CHANNELS

Table I summarizes the trajectory calculations carried out for the $HS(v', j' = 1) + O_2(v'' = 0, j'' = 1)$ reaction. First entry of this table indicates the

vibrational quantum number of the HS radical while the studied translational energies are in column 2. In this paper, we are interested essentially in the loss of HS, and therefore the last four columns of the table show values of the specific total reactive cross section and its associated uncertainties, independently of the determined reactive channel followed in the reactive collision.

Considering the energetic barriers of transitions states TS_3, TS_5, and TS_4 all channels are closed for low translational energies when vibrational states of the reactants are fixed at the ground levels. For total energies below 28.5 kcal mol^{-1}, the HSO channel remains practically closed and the only formed species is SO_2, following the path in Figure 2, with a relatively small cross section values. For higher total energies, the HSO channel opens (following the path illustrated in Fig. 1) and this species becomes the dominant product. Such a result is explained considering that the formation of HSO requires to break and form only one bond, whereas the SO_2 production requires more structural rearrangements (see Fig. 2). Contrarily, when the total energy of colliding molecules is above the HS dissociation limit for excited states of the HS radical with vibrational quantum number $v' = 7$ and translational energies greater than 25 kcal mol^{-1}, the formation of SO_2 dominates, because of the possibility of rupture of the HS radical followed by capture of the S atom by the unbroken O_2 molecule becomes significant. Nevertheless the above mentioned species are the major products of reaction (4); other reactive channels are also energetically allowed, but a detailed analysis of all reactive channels is out of the scope of the present work and will be hopefully reported in the forthcoming paper.

In this work, tunneling will not be considered, and of course a rigorous study of the title reaction requires quantum dynamics calculations, but regarding the characteristics of our PES and the energetic position of the main product here obtained such effect should not affect the final results in remarkable way. More important can be the well-known problem of classical trajectories called zero-point energy (ZPE) leakage. Several strategies divided into two groups: "active" and "nonactive" methods, have been proposed to deal with this problem [41]. In the active methods, a constraint is introduced to prevent the trajectories from entering the region of phase space, which allows vibrational modes to have less than its ZPE. Instead, the nonactive ones follow the genuine QCT approach but discard from the statistics any unphysical trajectory that is found to violate some specified physical criteria. The perturbed statistics may eventually be corrected *a posteriori*. Clearly, the mentioned procedures are not free from ambiguity and we use in this work only the nonactive internal energy quantum mechanical threshold (IEQMT) [41] method to compare with the pure QCT results. In the IEQMT method, a trajectory is not considered in the statistical analysis unless each molecular product has an internal energy larger than its corresponding ZPE. Thus, some trajectories accounted in QCT calculations, reaching unphysical products with internal energy bellow its ZPE, will be disregarded once the IEQMT criteria is used.

In the fourth and fifth columns of Table I, total and reactive trajectories number according the IEQMT criteria are shown. The sixth column collects the reactive trajectories according to QCT calculations. From detailed analysis of trajectories results shown in Table I, one verifies that reactive trajectories number is little affected by accounting (IEQMT) or not (QCT) ZPE. This result may be rationalized from analyzing the reaction mechanism by following some reactive trajectories step by step. At low translational energies, as we mentioned earlier, the reaction proceeds via path showed in Figure 2, the newly formed SO_2 has a large vibrational energy, and therefore, the number of reactive trajectories will not be affected by the way used to account ZPE. For higher translational energy, the title reaction is more likely to occur via path in Figure 1, and therefore, HS bond remains almost as an spectator, keeping its vibrational energy same as in the beginning of the collisional process. However, the SO and OO bonds continue interchanges of energies resulting in a vibrationally excited SO bond when the oxygen atom leaves the moiety. Then the vibrational energy of the products will more likely be above its ZPE. The major influence of ZPE leakage is observed for the nonreactive trajectories when the colliding molecules are not vibrationally excited. Despite disregarding such trajectories from the final statistics might imply that reactivity will be overestimated with respect to the traditional QCT values, we simply discard all trajectories not fulfilling the threshold condition of IEQMT method without any attempt to improve the statistics *a posteriori* considering that the mentioned criteria retains acceptable statistics and compares well with QCT approximation. Of course, such approach led to upper (IEQMT) and lower (QCT) values for cross section and, then, for rate constants.

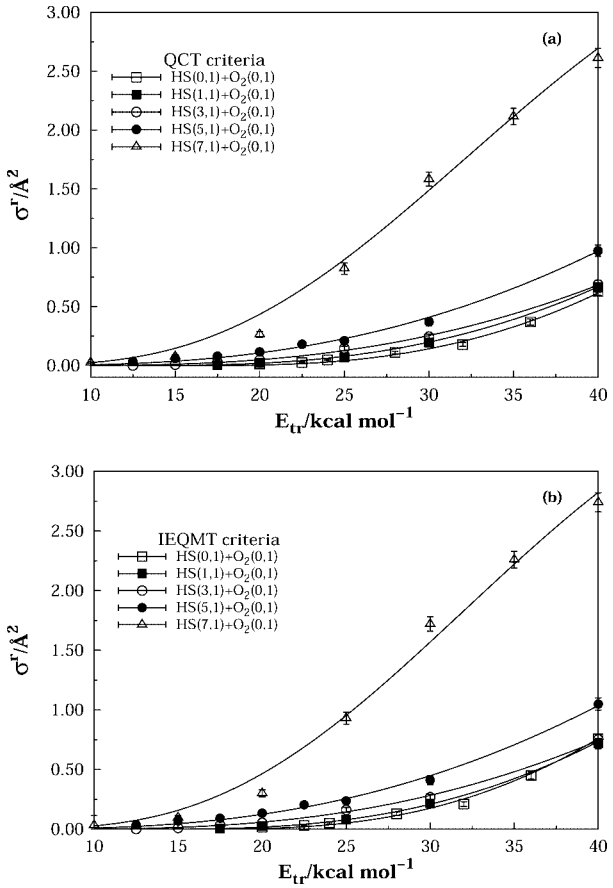

FIGURE 3. Specific total reactive cross section. Graph (a) shows the QCT results; graph (b) shows the IEQMT results.

4.2. REACTIVE CROSS SECTIONS

We now examine the shape of the excitation functions (cross section vs. translational energy) for any product formation, shown in Figure 3. Graph (a) of this figure displays obtained results when using the QCT calculations, whereas cross section obtained by using the IEQMT criteria are shown in graph (b). For all initial energetic conditions one observes the common pattern found in reactions which have an energy threshold; i.e., σ^r is an increasing function of $E_{\rm tr}$ for translational energies above the value $E_{\rm tr}^{\rm th}$, while the reactive channels remain practically closed for $E_{\rm tr}$ below the mentioned threshold. As expected, such a threshold decreases when internal energy is added to the reactants.

To analytically describe the dependence of the cross section with the translational energy, we have adopted the form [35]

$$\sigma^r_{\xi,0}(E_{\rm tr}) = C(\xi)\big[E_{\rm tr} - E_{\rm tr}^{\rm th}(\xi)\big]^n \exp\big\{-m\big[E_{\rm tr} - E_{\rm tr}^{\rm th}(\xi)\big]\big\}. \tag{8}$$

To consider the effect of internal energy we have now introduced the polynomials

$$C(\xi) = b_0 + b_1\xi + b_2\xi^2 \tag{9}$$

and

$$E_{\rm tr}^{\rm th}(\xi) = a_0 + a_1\xi + a_2\xi^2 + a_3\xi^3 \tag{10}$$

where

$$\xi = \frac{E_{\rm int}^{\rm HS} - E_{\rm int}^{\rm HS(v'=0,1)}}{E_{\rm int}^{\rm HS(v'=0,1)} + E_{\rm int}^{\rm O_2(v''=0,1)}}. \tag{11}$$

The parameters and coefficients in Eqs. (8)–(10) have been determined from two least-squares fitting procedures, one for vibrational quantum number $v' = 7$ when the formation of SO_2 is dominant and the other for remained combinations of vibrational quantum numbers for which the major product is the HSO; their optimum numerical values are reported in Table II. The resulting fitted functions are shown together with the calculated points in Figure 3. It is seen that the model reflects the general trends of the calculations. Note that the representation depends only on the internal energy of the reactants species, but not on any specific model that express the dependence of the internal energy with the quantum numbers. For a more detailed model, one would need further trajectory calculations covering a wide range of rovibrational states of the reactants. Of course, experimental information would also enlighten this topic. Note also that there are no qualitative differences between curves in graphs (a) and (b) of the Figure 3, but curves in graph (b) obtained with the IEQMT approach show values of the reactive cross sections slightly higher that those in graph (a) calculated with the QCT method.

By substitution of Eq. (8) in Eq. (7) and performing the integration analytically, the specific reactive thermal rate coefficient $k^r_{v',0}(T)$ assumes the form

$$k^r_{v',0}(T) = g_e(T)C(\xi)\left(\frac{8}{\pi\mu}\right)^{1/2} \times \frac{(k_BT)^{n+1/2}}{(1+mk_BT)^{n+2}} \exp\left(-\frac{E_{\rm tr}^{\rm th}}{k_BT}\right) \times \left[\Gamma(n+2) + \Gamma(n+1)(1+mk_BT)\frac{E_{\rm tr}^{\rm th}}{k_BT}\right] \tag{12}$$

TABLE II

Numerical values[a] for coefficients of the cross section functions.

Coefficient cross section	QCT $v' = 0 - 5$	QCT $v' = 7$	IEQMT $v' = 0 - 5$	IEQMT $(v' = 7)$
a_0	16.063	15.0845	16.0646	16.0635
a_1	−3.3609	−2.07762	−2.06134	−2.08934
a_2	0.406581	−0.396197	−0.275666	−0.507805
a_3	−0.0312129	0.0563436	0.0443081	0.0687352
b_0	8.5329×10^{-5}	0.000131026	0.000105283	0.000117139
b_1	-2.0340×10^{-5}	0.000185255	-2.84146×10^{-5}	8.00128×10^{-5}
b_2	2.4166×10^{-6}	-2.67271×10^{-5}	3.23022×10^{-6}	-1.25883×10^{-5}
n	2.85843	4.98027	2.85843	4.98027
m	0.00800001	0.0886503	0.00800001	0.0886503

[a]The units are such that cross section is Å^2 and energy is kcal mol^{-1}.

where Γ is the gamma function. Figure 4 shows the function in Eq. (12) for vibrational quantum numbers 0, 1, 3, 5, and 7 of the HS radical. In graph (a) of Figure 4 have been included curves obtained with the QCT approach, whereas graph (b) has curves calculated with the IEQMT approximation. These graphics exhibit only small quantitative difference. As expected, all curves follow a similar pattern. At low temperatures they have small values, which are then rapidly increased when temperature is raised. The specific thermal rate coefficients increase with the initial vibrational state existing a difference of several orders of magnitude between these curves for low temperature. For high temperature the curves approach each other with a tendency to a plateau.

For completeness, we show the Arrhenius curves in Figure 5. The calculated vibrationally averaged thermal rate coefficient is given by

$$k^r(T) = \frac{\sum_{v'=0} \omega_{v'} k^r_{v',0}}{\sum_{v'=0} \omega_{v'}} \tag{13}$$

where vibrational populations $\omega_{v'}$ of HS are those obtained in the 193 nm photolysis of H_2S. For calculation of the upper limit curve the vibrational population was taken from Ref. 3 and for the lower limit curve from Ref. 7. Calculations using the vibrational population reported in Refs. 2, 4–6, and 8 lead to intermedial values.

We now turn to the available experimental data [10–16]. As was already mentioned, only upper limits have been experimentally reported for the title reaction at room temperature. Such results have been also included in Figure 4. The IUPAC recommended value for the rate coefficient is the lowest upper limit obtained by Stachnik and Molina [15] in a flash photolysis/UV absorption study of the reaction of HS radicals with O_2. The source of HS radicals in this experiment was the photodissociation of H_2S with pulsed ArF excimer laser emission at 193 nm. Despite, as was admitted by the authors of this work, the H_2S radical has high quantum yield of HS($v' = 0$)

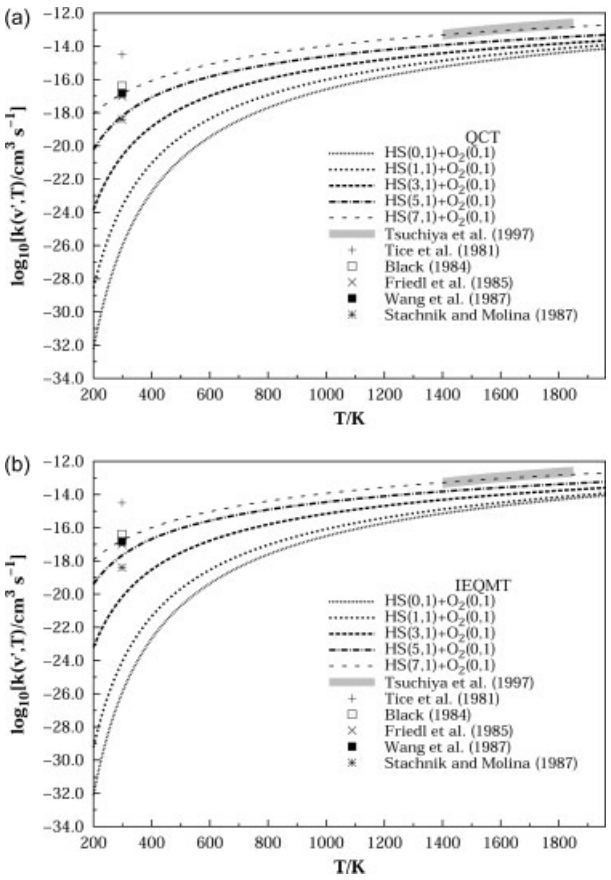

FIGURE 4. Specific thermal total reactive rate coefficients. Graph (a) shows the QCT results, graph (b) shows the IEQMT results.

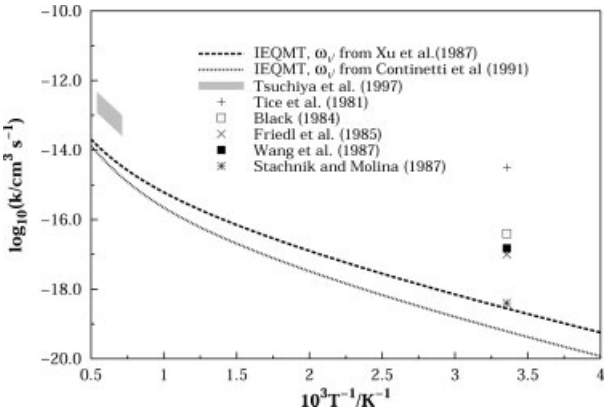

FIGURE 5. Arrhenius plots for the rate coefficients of the title reaction. Averaged IEQMT rate constants using two different populations for vibrational levels of HS reported in literature are compared with the experimental results.

at 193 nm, HS radicals in other vibrational states are also produced under the same experimental conditions [2–8]. Thus, it could be interesting to consider the possible participation in the reaction of such vibrational excited radicals. The relative high pressure of oxygen (730 Torr) utilized in this experiment is not a warranty of quenching because the reactive and relaxation processes are competitive ones and the final result depends on the ratio of rate coefficients of both processes, but unfortunately we are unaware of works devoted to relaxation studies of vibrationally excited HS by O_2.

Rate coefficients for the title reaction at high temperature were reported in Ref. 17, and they have been included in Figures 4 and 5. In this study, the HS radical was produced also by laser photolysis at 193 nm of a mixture of H_2S and O_2 highly diluted in Ar. Note that with the indicated wave length the O_2 is also photolyzed. Note also that the situation allows an effective production of vibrationally excited HS radicals. In these experiments, the rate constants were measured by monitoring the time dependencies of both O and H atoms assuming the HSO + O as dominant products. Under these experimental conditions an overestimation of rate constant values could be expected and, as was admitted by the authors, "the accuracy of the rate constants obtained in this study is not clear" [17]. We want to remark the good agreement of the experimental results with our evaluation of rate coefficients for the highest vibrationally excited HS radicals showed in graph (a) of Figure 4 for which is obtained the most intensive reaction, although graph (b) shows that reported coefficients at high temperature lies above calculations. Such a result is consistent with the previous analysis leading to the criteria of an experimental overestimation of the rate coefficients at high temperatures. At room temperature there exists agreement between our average rate coefficients and the IUPAC recommended measurements by Stachnik and Molina [15] considering that it is an upper limit for rate coefficient.

In a theoretical study by Goumri et al. [18], the G2 method and RRKM theory were used to analyze the rate constant for reaction (3). An evaluation of the reverse reaction leads to a bimolecular rate constant of 2.3×10^{-14} cm^3 s^{-1} [30], which is much larger than the rate constants provided experimentally. More recently the mentioned reaction was investigated using single- and multi-reference theoretical techniques [30]. In such a work, authors conclude that dissociation of HSOO into HSO+O and H+SOO are very endothermic and nonspontaneous processes; therefore, they may be neglected at atmospheric conditions. Moreover, authors indicate that H + SO_2 is not produced in the reaction of HS+O_2 because they found that it is not a one-step process. For the ground vibrational state we have arrived to similar conclusions: the major product is the HSO radical and the specific rate coefficients for relevant atmospheric temperatures are extended in the interval of 1.0×10^{-32} to 1.0×10^{-26} cm^3 s^{-1}. However, our calculations led to very different results for vibrationally excited HS radicals, and thus we could support theoretically the relative high experimental values reported in the work by Stachnick and Molina [15]. In relation with the processes occurring in the atmosphere they must be analyzed carefully because events with a very low reactive cross section in normal conditions, due to having a high endoergicity, could be relevant for the study of atmospheric chemistry considering the existence of vibrationally hot species under conditions of nonlocal thermodynamic equilibrium makes possible the occurrence of endoenergetic reactions which would not be possible otherwise [42]. The next work will be addressed to that problem.

5. Conclusions

A theoretical study of the title reaction was carried out by means of QCT method, for a wide range of translational energies of the reactants. The use of a global PES for HSO_2 allows to explore the reaction mechanism. SO_2 and HSO were the most obtained species, with significant differences on their rate

coefficients. The latter is the most favored product once it is energetically reachable. Influence of the vibrational excitation of HS radical on the reaction was accounted by carrying out calculations for different vibrational quantum numbers ($v' = 0, 1, 3, 5, 7$). Cross sections were reported. The title reaction shows a barrier-like behavior. A model to account the internal energy of the reactants was also presented. ZPE leakage was considered by demanding the internal energy of each of the products to be above their respective ZPE, and disregarding all trajectories not fulfilling such a condition. Rate coefficients were analytically obtained and compared with values reported in literature. The vibrational energy of HS plays a significant role, and the good agreement of rate coefficients here reported with the recommended values in literature is obtained when vibrationally excited populations of HS are considered. These results could point out to the necessity of to consider the vibrational excitation of HS radicals for understanding experimental data. The relevance of the mentioned issues for atmospheric chemistry requires a more detailed analysis including the evaluation of relaxation processes.

ACKNOWLEDGMENT

M.Y.B thanks Centro de Estudios Ambientales de Cienfuegos (CEAC), Cuba, for leave of absence during his Ph.D. studies.

References

1. Wayne, R. P. Chemistry of Atmospheres; Oxford University Press: Oxford, 2002.
2. van Veen, G. N. A.; Mohamed, K. A. A.; Baller, T.; de Vries, A. E. Chem Phys 1983, 74, 261.
3. Xu, Z.; Koplitz, B.; Wittig, C. J Chem Phys 1987, 87, 1062.
4. Weiner, B. R.; Levene, H. B.; Valentini, J. J.; Baronavski, A. P. J Chem Phys 1989, 90, 1403.
5. Schnieder, L.; Meier, W.; Welge, K. H.; Ashfold, M. N. R.; Western, C. M. J Chem Phys 1990, 92, 7027.
6. Xie, X.; Schnieder, L.; Wallmeier, H.; Boettner, R.; Welge, K. H.; Ashfold, M. N. R. J Chem Phys 1990, 92, 1608.
7. Continetti, R. E.; Balko, B. A.; Lee, Y. T. Chem Phys Lett 1991, 182, 400.
8. Liu, X.; Hwang, D. W.; Yang, X. F.; S. Harich, J. J. L.; Yang, X. J Chem Phys 1999, 111, 3940.
9. Leu, M.-T.; Smith, R. H. J Phys Chem 1982, 86, 73.
10. Sze, N. D.; Ko, M. Atmos Environ 1980, 14, 1223.
11. Tice, I. J.; Wampler, F. B.; Oldenborg, R. C.; Rice, W. W. Chem Phys Lett 1981, 82, 80.
12. Black, G. J Chem Phys 1984, 80, 1103.
13. Friedl, R. R.; Brune, W. H.; Anderson, J. G. J Phys Chem 1985, 89, 5505.
14. Schoenle, G.; Rahman, M. M.; Schindler, R. N.; Busenges, B. Phys Chem 1987, 91, 66.
15. Stachnick, R. A.; Molina, M. J. J Phys Chem 1987, 91, 4603.
16. Wang, N. S.; Lovejoy, E. R.; Howard, C. J. J Phys Chem 1987, 91, 5743.
17. Tsuchiya, K.; Kamiya, K.; Matsui, H. J Chem Kinet. 1997, 29, 57.
18. Goumri, A.; Rocha, J.-D. R.; Marshall, P. J Phys Chem 1995, 99, 10834.
19. Binns, D.; Marshall, P. J Chem Phys 1991, 95, 4940.
20. Morris, V. R.; Jackson, W. M. Chem Phys Lett 1994, 223, 445.
21. Laakso, D.; Smith, C. E.; Goumri, A.; Rocha, J.-D. R.; Marshall, P. Chem Phys Lett 1994, 227, 377.
22. Frank, A. J.; Sadílek, M.; Ferrier, J. G.; Tureček, F. J Am Chem Soc 1996, 118, 11321.
23. Qi, J.-X.; Deng, W.-Q.; Han, K.-L.; He, G.-Z. J Chem Soc Faraday Trans 1997, 93, 25.
24. Frank, A. J.; Sadílek, M.; Ferrier, J. G.; Tureček, F. J Am Chem Soc 1997, 119, 12343.
25. Isoniemi, E.; Kriadchtchev, L.; Lundell, J.; Rasanen, M. J Mol Struct 2001, 563–564, 261.
26. Isoniemi, E.; Kriadchtchev, L.; Lundell, J.; Rasanen, M. Phys Chem Chem Phys 2002, 4, 1549.
27. Goumri, A.; Rocha, J.-D. R.; Laakso, D.; Smith, C. E.; Marshall, P. J Phys Chem A 1999, 103, 11328.
28. Denis, P. A.; Ventura, O. N. Chem Phys Lett 2001, 344, 221.
29. Ballester, M. Y.; Varandas, A. J. C. Phys Chem Chem Phys 2005, 7, 2305.
30. Resende, S. M.; Ornellas, F. R. Phys Chem Chem Phys 2003, 5, 4617.
31. Varandas, A. J. C. In Lecture Notes in Chemistry, Vol. 75: Reaction and Molecular Dynamics; Laganá, A.; Riganelli, A., Eds.; Springer: Berlin, 2000; p 33.
32. Hase, W. L. Encyclopedia of Computational Chemistry; Wiley: New York, 1998.
33. (a) Hase, W. L. MERCURY: A general Monte-Carlo classical trajectory computer program. QCPE 1983, 3, 453; (b) Hase, W. L.; Duchovic, R. J.; Hu, X.; Komornik, A.; Lim, K. F.; Lu, D.-H.; Peslherbe, G. H.; Swamy, K. N.; van de Linde, S. R.; Varandas, A. J. C.; Wang, H.; Wolf, R. J. VENUS96 (an updated version of MERCURY). QCPE Bull 1996, 16, 43.
34. Varandas, A.; Pais, A.; Marques, J.; Wang, W. Chem Phys Lett 1996, 249, 264.
35. Garrido, J. D.; Caridade, P. J. S. B.; Varandas, A. J. C. J Phys Chem A 1999, 103, 4815.
36. Ballester, M. Y.; Varandas, A. J. C. Chem Phys Lett 2007, 433, 279.
37. Karplus, M; Porter, R. N.; Sharma, R. D. J Chem Phys 1965, 43, 3259.
38. Truhlar, D. G. J Chem Phys 1972, 56, 3189.
39. Muckerman, J. T.; Newton, M. D. J Chem Phys 1972, 56, 3191.
40. Huber, K. P.; Herzberg, G. Constants of Diatomics Molecules; Van Nostrand: Princeton, 1979.
41. Varandas, A. J. C. Chem Phys Lett 1994, 225, 18.
42. Guerrero, Y. O.; Garrido, J. D. Revista Cubana de Física 2006, 22, 45.